

Short Communication

## Study on Microstructure and Corrosion Resistance of Duplex Stainless Steel 2205 in Real Seawater Rich containing Mold

Qiuxia Ran<sup>1</sup>, Jingyu Guo<sup>2</sup>, Zilong Zhao<sup>3,\*</sup>, Baoyu Duan<sup>4,\*</sup>, Lining Fang<sup>5</sup>, Liang Li<sup>6</sup>

<sup>1</sup> School of Urban Economics, Lanzhou City University, 730070, China

<sup>2</sup> Sino-French Institute of Nuclear Engineering and Technology, Sun Yat-sen University, Zhuhai 519082, China

<sup>3</sup> School of Chemical Engineering and Technology, Sun Yat-sen University, Zhuhai 519082, China

<sup>4</sup> Analysis and Testing Center, Inner Mongolia University of Science and Technology, Baotou 014010, China.

<sup>5</sup> Hebei University of Environmental Engineering

<sup>6</sup> School of Physics, Engineering and Computer Science, University of Hertfordshire, Hatfield AL10 9AB, UK

\*E-mail: [rqx@lzcw.edu.cn](mailto:rqx@lzcw.edu.cn), [zhaozlong@mail.sysu.edu.cn](mailto:zhaozlong@mail.sysu.edu.cn), [77867350@qq.com](mailto:77867350@qq.com)

Received: 20 March 2022 / Accepted: 22 April 2022 / Published: 6 June 2022

---

2205 duplex stainless steel (DSS) has been widely used in the marine environment because of its excellent corrosion resistance. The moist and hot environment of the ocean is suitable for the growth and reproduction of microorganisms, especially mold, which cause serious corrosion problems. In this paper, the seawater extracted from the South China Sea with abundant microorganisms was used as a test medium, and mold isolated from the Xisha Sea area of China was added. The microstructure and corrosion behavior of 2205 DSS were studied by using EBSD, 3D optical microscopy, electrochemical workstation, and SEM. The corrosion mechanism of 2205 DSS with different textures and grain orientation in seawater containing microorganisms was systematically analyzed.

---

**Keywords:** 2205 stainless steel, Microbial corrosion, Microstructure, Mold

### 1. INTRODUCTION

Corrosion is the main factor leading to facility failure [1, 2]. Various corrosion control technologies have been developed, such as coatings, corrosion inhibitors, and cathodic protection, as well as alloys with excellent corrosion resistance[3-6]. Stainless steel and acid-resistant steel have been widely used in the field of corrosion prevention. Stainless steel is a kind of steel with high corrosion resistance in weakly corrosive media such as air and freshwater. Acid resistant steel refers to the steel

with corrosion resistance in harsh corrosive media, such as acid, alkali, salt, and seawater. The results show that the corrosion resistance of steel increases with the increase of the content of Cr. When the content of Cr exceeds 12%, the corrosion resistance of steel in the atmosphere changes from weak to strong. The corrosion resistance of stainless steel is due to the formation of a passivation film on its surface. The chemical composition, structure and properties of passivation film vary with the chemical composition and treatment methods of stainless steel and the medium environment. Chrome stainless steel is equivalent to the AISI400 series in the United States. Chromium stainless steel includes ferritic stainless steel, representative grade 409, 430, etc. Elements that enable the steel to form ferrite include Cr, Mo, Si, Al, W, Ti, Nb and so on. In the 1880s, people found austenite in middle and high carbon steel at high temperature, after fast cooling to get a steel hardening and strengthening of the organization, later developed martensitic stainless steel, on behalf of 410,431 and so on. The main alloying elements of chrome-nickel stainless steel are chromium and nickel, which is equivalent to the AISI300 series in the United States. The elements that enable the steel to form austenite include Ni, C, N, Mn, Cu, etc., representing grades 304, 316, etc. The development and application of DSS began in the 1930s, and France obtained the first patent in 1935. In the solid solution structure of DSS, the ferrite phase and austenite phase account for about half respectively, and generally the content of the small phase also needs not less than 30%. DSS combines the excellent toughness and weldability of austenitic stainless steel with the high strength and resistance to chloride and stress corrosion of ferritic stainless steel [7-9]. The first generation of DSS steel is represented by 329 steel developed in the 1940s in the United States. The widespread and extensive application of N in stainless steel is the most important progress in the field of stainless steel. In addition to ferritic stainless steel, almost all types of stainless steel, especially austenitic and DSS are commonly alloyed with N. N was added to the DSS to develop the second generation (representative grade 2205) and third-generation (Super duplex stainless steel, representative grade SAF2507) of DSS. It not only significantly improves the corrosion resistance of austenitic and duplex stainless steels in oxidizing acid and reducing acid media, but also improves their resistance to local corrosion such as intergranular corrosion, and pitting corrosion, and crevice corrosion. In stainless steel, N improves pitting and crevice corrosion resistance by about 16-30 times that of chromium. Stainless steel is currently being used in more extreme environments, such as ultra-supercritical high temperature and high-pressure environments, stainless steel for nuclear power, and ultra-high pressure deep-sea environments [10, 11].

Microbiologically influenced corrosion (MIC) refers to the process of metal material corrosion accelerated directly or indirectly by microbial life activities and their metabolites [12]. The annual global cost of corrosion is about us 4 trillion dollars, of which microbial corrosion accounts for 20% [13, 14]. The resistance of stainless steel to MIC has been widely studied. Dec et al. [15] observed that sulfate-reducing bacteria could destroy the passive film of 2205 DSS by forming different sulfides, thus causing pitting corrosion. Liu has conducted a series of studies on MIC of carbon steel, stainless steel, and titanium alloys[16-20]. The hot and humid conditions of the ocean are ideal for the growth and reproduction of microorganisms, especially molds. 2205 DSS is widely used in the marine environment. However, the corrosion behavior of 2205 DSS in seawater medium with microorganisms has not been fully studied. In this paper, the microstructure and grain orientation of stainless steel 2205 was studied by EBSD. Then the seawater with mold was used as the test medium. The electrochemical corrosion

behavior of 2205 DSS for 14 days was tested by the electrochemical workstation. Finally, the morphology after corrosion was characterized by SEM. The corrosion mechanism of different textures and orientation grains in 2205 DSS in seawater containing microorganisms was analyzed.

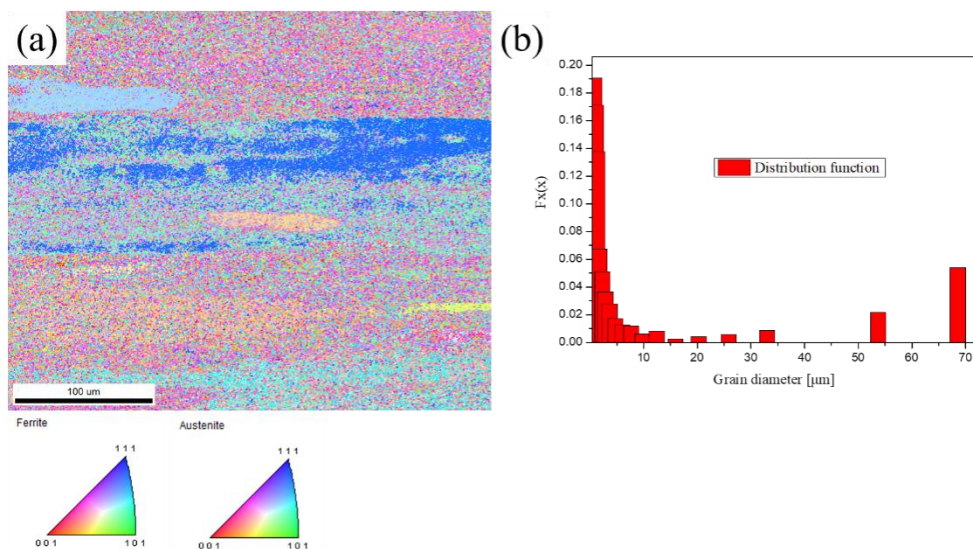
## 2. EXPERIMENTAL PROCEDURE

2205 commercial rolled plate (purchased from Baowu Tai Steel Group, the plate thickness of 10mm) is cut into corrosion coupons with a size of 10\*10\*10 mm for electrochemical testing and surface morphology characterization. The seawater containing marine microorganisms is obtained from the surface sea of Yangjiang, China. *Aspergillus terreus* isolated from Xisha sea area of China, and were used in this work [21]. The mold was cultured in a potato glucose liquid medium, and the composition (g/L) was glucose 20, NaCl 30, and potato juice 200. The medium was sterilized at 121 °C for more than 20 minutes before use and used to activate the mold after cooling. The mold needs to be cultured for 24 hours before the experiment.

The microstructures of the samples were examined by 3D Optical Microscopy (OM, LEICA DVM6), scanning electron microscope (SEM, JSM-7800 F, JEOL, Japan), Oxford electron backscatter diffraction (EBSD) system and energy dispersive spectrometer (EDS). The electrochemical corrosion process was studied using an electrochemical workstation (Model CS350, Corrtest, China).

## 3. RESULTS AND DISCUSSION

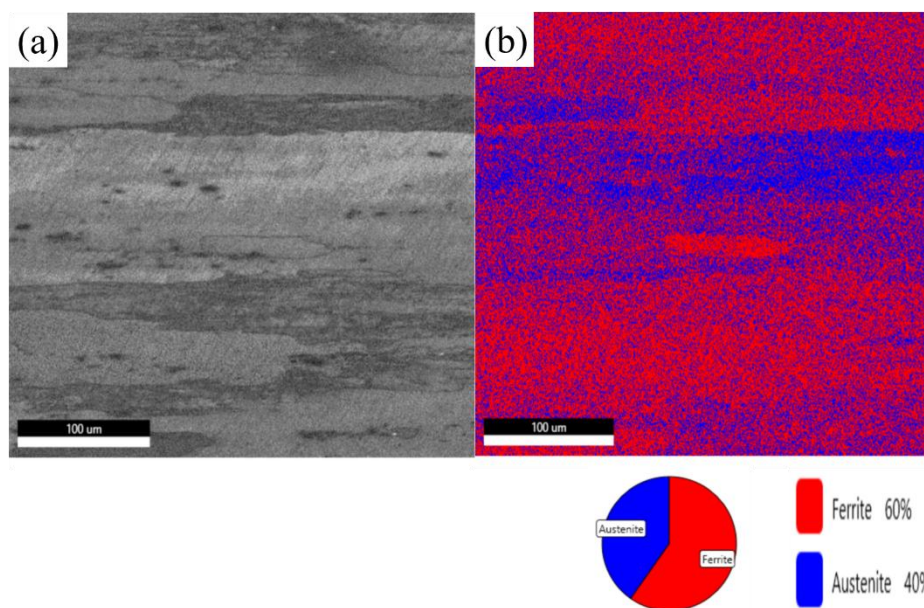
Fig. 1 is the EBSD characterization of the 2205 DSS rolled plate. Grain orientation mapping in Fig. 1a shows that grains are distributed in all orientations, among which there are more grains in the plane (001) and plane (111), which is mainly the result of base rolling and preferred orientation.



**Figure 1.** EBSD analysis of 2205 rolled plate: (a) Grain orientation mapping. (b) grain size distribution.

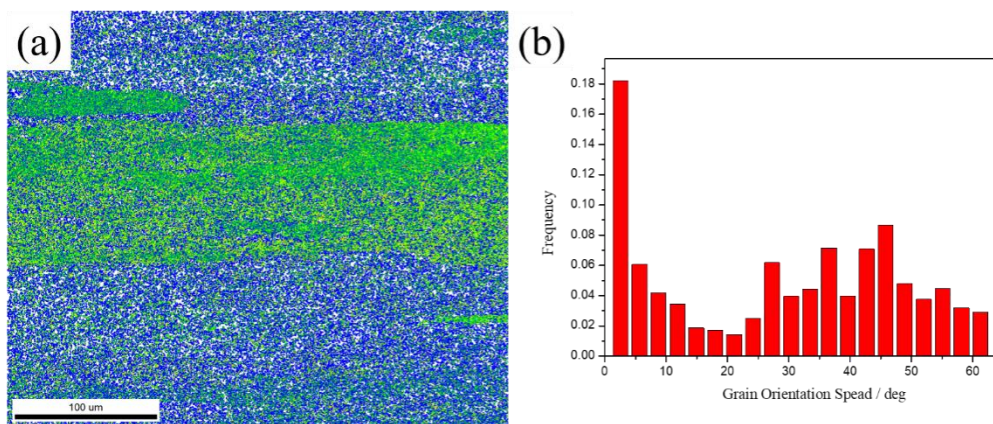
It can be seen from Fig. 1b that there are many grains with a diameter of fewer than 10 μm, and a few with a diameter of more than 30 μm, indicating that the material has a mixed crystal structure. The uneven grain distribution results in uneven corrosion resistance of materials. In the presence of microorganisms, corrosion occurs first at the grain boundaries of larger grains, cracking the metal grain boundaries and leading to failure.

Fig. 2 shows that austenite and ferrite phases are evenly distributed, with austenite accounting for 40% and ferrite for 60%. This uniform structure distribution combines the high strength of ferrite with the good plasticity of austenite, while reducing the cost of stainless steel by reducing the Ni content. The seawater corrosion resistance of the material is better than 316L SS [22], which is great progress in the field of seawater corrosion resistant stainless steel. As can be seen from Fig. 1, ferrite is mainly (001) plane grain, which is mainly due to the strong texture of the base plane, which is caused by the poor plasticity of ferrite. The austenite is mainly (111) plane grain, which is mainly caused by better plasticity and preferred orientation of austenite.



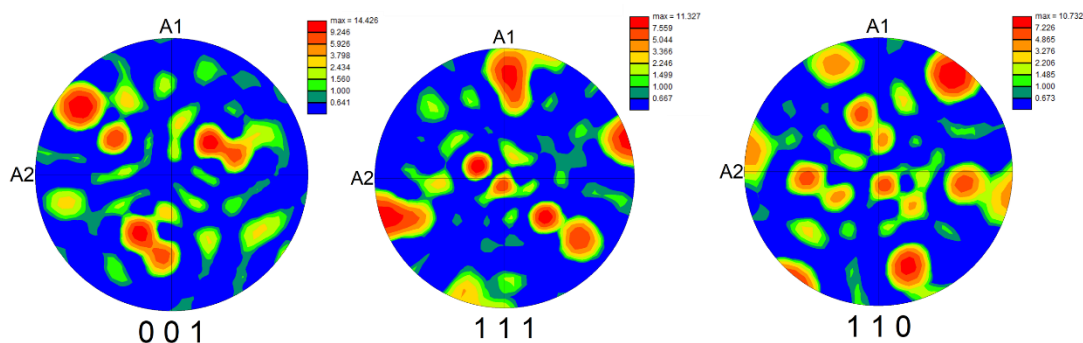
**Figure 2.** (a) SEM of 2205 rolled plate (b) Different types of grains in the alloy; blue and red color represent austenite, and ferrite grains, respectively.

Fig. 3 shows grain frequency of 2205 rolled plate orientation Angle. It can be seen from the images that the distribution proportion of small angle grain and large angle grain is similar, which is related to the isotropy of austenitic stainless steel and ferritic stainless steel polycrystal, indicating that the grains of duplex stainless steel is below 70 degrees, and the proportion is similar.



**Figure 3.** grain frequency of 2205 rolled plate orientation angle: (a) Kernel average misorientation (b) grain frequency of orientation angle.

Fig. 4 shows grain frequency of 2205 rolled plate orientation Angle. It can be seen from the figure that (001) has the highest strength of 14.426, which is caused by the base surface of ferritic stainless steel in the rolled surface. The strength of plane (111) and plane (110) is also unevenly distributed due to different grain orientations. The strength of (111) is mainly contributed by austenitic stainless steel, which corresponds to the microstructure of Fig.1 and Fig.2.



**Figure 4.** Pole figure analysis of 2205 rolled plate.

The electrochemical results of 2205 DSS tested continuously for 14 days in surface seawater containing mold are shown in Fig. 5. It can be seen from Fig. 5 that the impedance value of DSS increased and then decreased on the second day, indicating that the corrosion of DSS was a process of corrosion and repair at the same time and that the seawater containing mold and other microorganisms had strong corrosion ability. MIC is a long-term and complex process. Generally, microorganisms first attach to the surface of the material and then release acidic metabolites to accelerate the corrosion. Then, the metabolites form biofilms, resulting in a large area of electrochemical corrosion galvanic cells to further accelerate the corrosion of the alloy [23-26]. Therefore, the impedance value of 2205 DSS begins to decrease after soaking for 2 days. However, it is still seen that the impedances changed little with time,

and the impedance values were big. So, this suggests that 2205 DSS has higher corrosion resistance in the seawater due to the good passive film [27, 28].

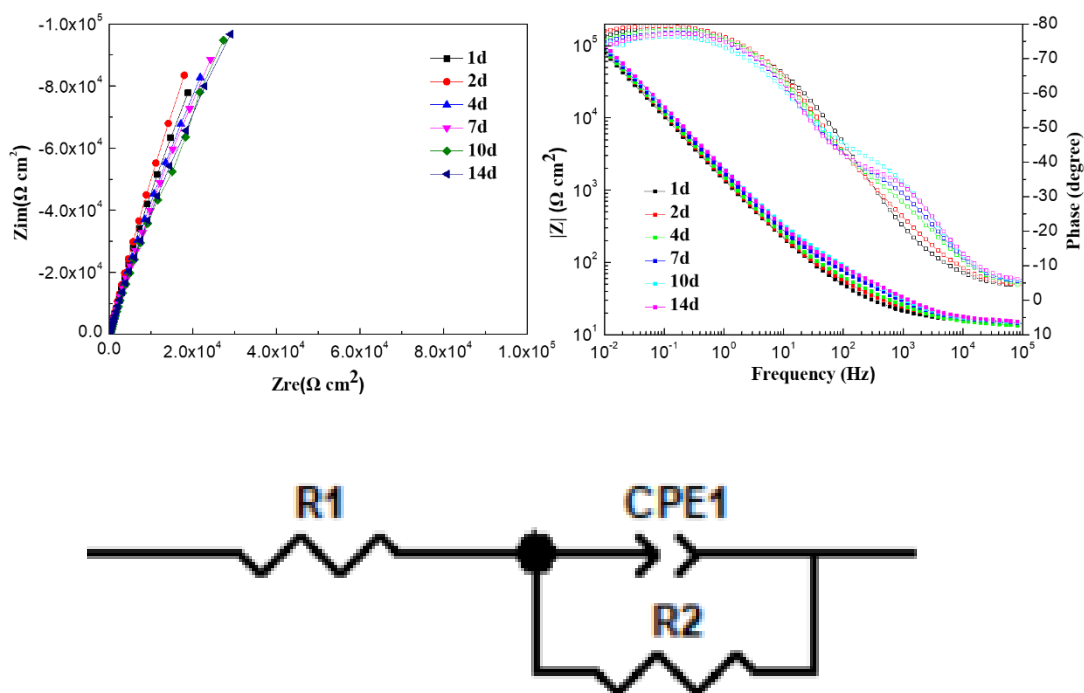


**Figure 5.** Electrochemical Impedance Spectroscopy (EIS) plots obtained on seawater containing mold. The figure below demonstrates the equivalent circuits applied to fit EIS plots.

**Table 1.** The EIS data from Figure 5 are fitted using the fitting circuit

	$R_s$	CEP-T	CEP-P	$R_t$
1 d	10.4	$5.66 \times 10^{-5}$	0.80	$6.38 \times 10^{-6}$
2 d	10.22	$4.51 \times 10^{-5}$	0.82	$7.92 \times 10^{-6}$
4 d	11.1	$2.91 \times 10^{-5}$	0.85	$2.94 \times 10^{-6}$
7 d	10.09	$5.07 \times 10^{-5}$	0.83	$5.38 \times 10^{-6}$
10 d	11.15	$6.08 \times 10^{-5}$	0.80	$9.59 \times 10^{-6}$
14 d	10.97	$6.03 \times 10^{-5}$	0.80	$7.53 \times 10^{-6}$

Fig. 6 shows Optical Microscopy images of 2205 rolled plate after corrosion in seawater containing mold. It can be seen from Fig. 6a and Fig. 6b that 2205 stainless steel has a small amount of white microbial products on its surface after corrosion in seawater. Combined with the THREE-DIMENSIONAL morphology of Fig. 6c and Fig. 6d, it can be seen that there are tiny corrosion holes on the surface, indicating that the corrosion type of 2205 stainless steel within 14 days is localized corrosion. It has been reported that the corrosion resistance of austenitic stainless steel in seawater is poor [29], so the corrosion holes occur in the austenite area. In general, the 2205 stainless steel showed strong

corrosion resistance in the seawater containing microorganisms for 14 days, but the mold promoted localized corrosion, forming corrosion holes on the surface and leading to the failure of the stainless steel.

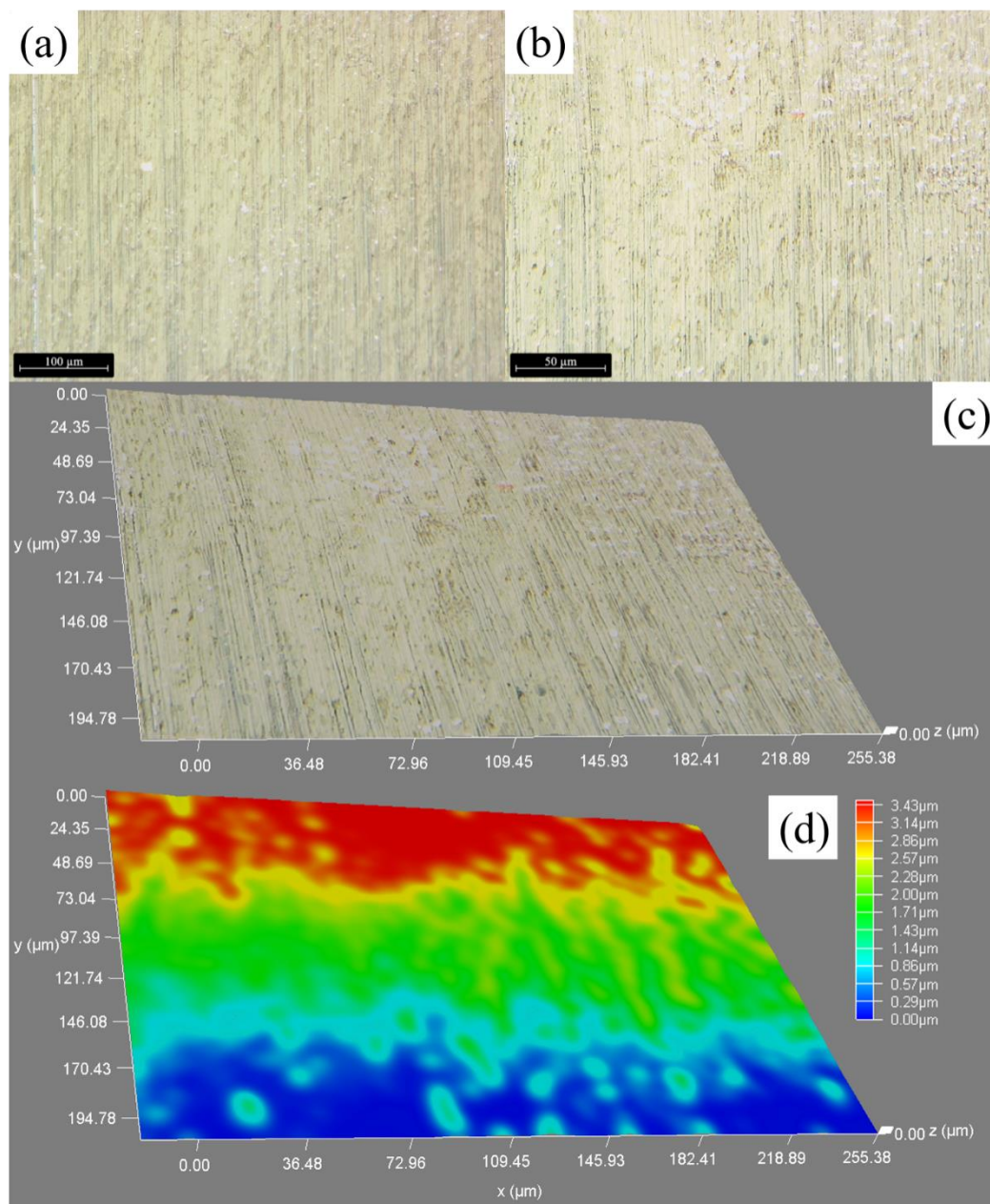


**Figure 6.** Optical Microscopy images of 2205 rolled plate after corrosion in real seawater containing mold. (a) and (b) is the optical microscopy image. (c) and (d) are the 3D reconstruction of figure (b).

The morphology and phase composition of the corrosion products were further studied. The morphology of 2055 stainless steel in seawater containing mold after corrosion was characterized by SEM image and EDS. Fig. 7a and Fig. 7b obviously showed that there were many corrosion pits. This is consistent with the results in Fig. 6. Combined with EDS, it can be found some inclusions. The presence of inclusion can easily cause pitting corrosion, and the growth location of corrosion pits is

usually around the inclusion [30]. Fungi, such as the molds, have been considered as one of the key reasons for accelerating the steel corrosion, especially for the localized corrosion [31, 32]. So, it can be speculated that the localized corrosion of 2055 stainless steel can be caused by the multi-factors.

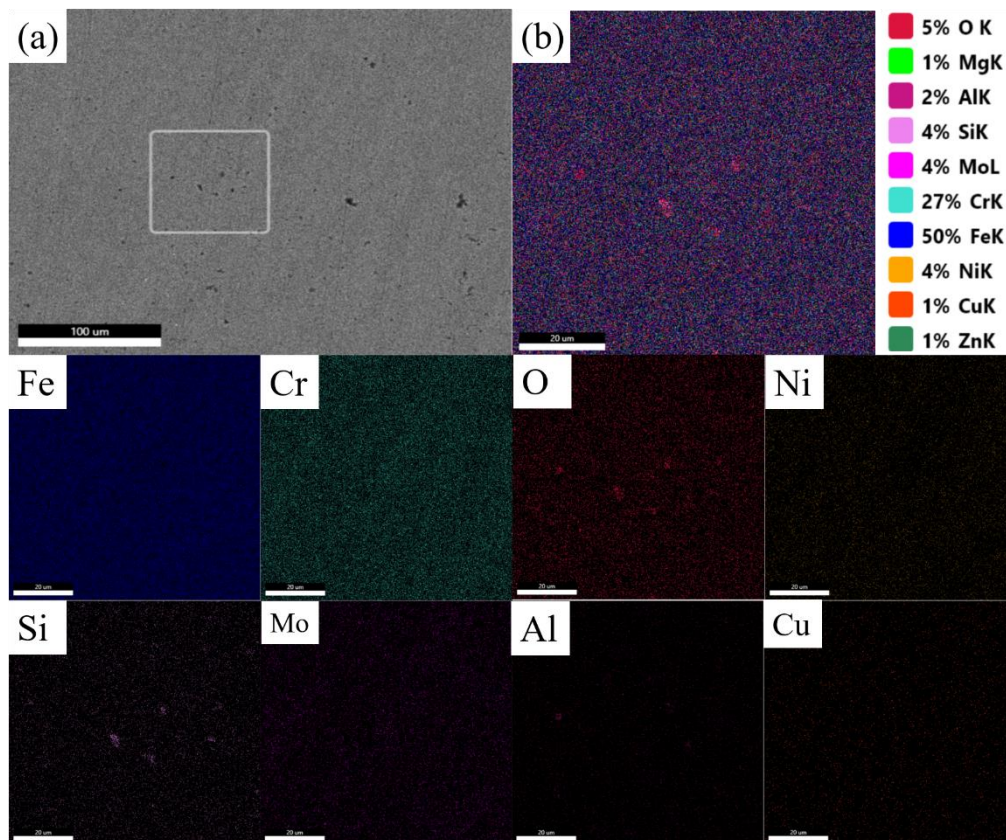


Figure 7. SEM image and EDS of 2205 rolled plate after corrosion in real seawater containing mold.

#### 4. CONCLUSION

1. Ferrite is mainly (001) plane grain, which is mainly due to the strong texture of the base plane, which is caused by the poor plasticity of ferrite. The austenite is mainly (111) plane grain, which is mainly caused by better plasticity and preferred orientation of austenite.

2. 2205 stainless steel has demonstrated strong corrosion resistance in the seawater environment containing mold for 14 days, but mold will promote the localized corrosion intensification, forming corrosion holes on the surface to make the stainless steel failure.

3. The main components of corrosion holes are Si and O, indicating that the main factor causing corrosion holes is mold.

#### ACKNOWLEDGEMENTS

This work was supported by 2019, Gansu Province Philosophy and Social Science Planning Project, No. 19YB078



## References

1. H. W. Liu, D. K. Xu, K. Yang, H. F. Liu and Y. F. Cheng, *Corros Sci.*, 132 (2018) 46.
2. Z. Feng, C. C. Xu, D. Zhang and R. Buchheit, *Materials*, 14 (2021) 286.
3. D. Sun, D. Xu, C. Yang, J. Chen, M. B. Shahzad, Z. Sun, J. Zhao, T. Gu, K. Yang and G. Wang, *Mater. Sci. Eng. C*, 69 (2016) 744.
4. T. Xi, C. G. Yang, M. B. Shahzad and K. Yang, *Mater Design*, 87 (2015) 303.
5. Z. Y. Feng, B. Hurley, J. C. Li and R. Buchheit, *J Electrochem Soc.*, 165 (2018) C94.
6. Z. Y. Feng, B. Hurley, M. L. Zhu, Z. Yang, J. Hwang and R. Buchheit, *J Electrochem Soc.*, 166 (2019) C520.
7. H. Tan, Y. Jiang, B. Deng, T. Sun, J. Xu and J. Li, *Mater Charact.*, 60 (2009) 1049.
8. Y. Yang, H. Zeng, S. Xin, X. Hou and M. Li, *Corros Sci.*, 165 (2020) 108383.
9. Z. Zhao, X. Jiang, S. Li, L. Li, Z. Feng and H. Lai, *Crystals*, 12 (2022) 152.
10. Y. Pan, L. Song, Z. Liu, J. Hu and X. Li, *Corros Sci.*, 196 (2022) 10026.
11. Y. Fan, T. Liu, L. Xin, Y. Han, Y. Lu and T. Shoji, *J Nucl Mater.*, 544 (2021) 152693.
12. H. Liu and Y. F. Cheng, *Corros Sci.*, 173 (2020) 108753.
13. H. B. Li, E. Z. Zhou, D. W. Zhang, D. K. Xu, J. Xia, C. G. Yang, H. Feng, Z. H. Jiang, X. G. Li, T. Y. Gu and K. Yang, *Sci Rep.*, 6 (2016) 38854.
14. Z. Y. Feng, J. C. Li, Z. Yang and R. Buchheit, *Materials*, 13 (2020) 1325.
15. W. Dec, M. Mosialek, R. P. Socha, M. Jaworska-Kik, W. Simka and J. Michalska, *Electrochim. Acta*, 225 (2016) 212.
16. H. Liu and Y. F. Cheng, *Corros Sci.*, 133 (2018) 178.
17. H. W. Liu, T. Y. Gu, G. A. Zhang, H. F. Liu and Y. F. Cheng, *Corros Sci.*, 136 (2018) 47.
18. H. W. Liu, F. P. Xiong, L. Y. L., C. Y. Ge, H. F. Liu and Y. L. Hu, *J Chin Soc Corrosion&Protection*, 36 (2017) 645.
19. H. W. Liu, X. K. Zhong, H. F. Liu and Y. F. Cheng, *Electrochem Commun.*, 90 (2018) 1.
20. H. W. Liu, H. X. Liu and Y. X. Zhang, *Coatings*, 10 (2020) 1116.
21. Y. Zhang, J. He, L. Zheng, Z. Jin, H. Liu, L. Liu, Z. Gao, G. Meng, H. Liu and H. Liu, *npj Mater Degrad*, 6 (2022) 1.
22. H. Qin, Y. Gao, P. Liang and X. U. Ming, *Hot Working Tech.*, 12 (2015) 102.
23. Z. L. Zhao, Y. H. Li, Y. F. Zhong and Y. D. Liu, *Int J Electrochem Sci.*, 14 (2019) 6394.
24. Z. L. Zhao, Y. D. Liu, Y. F. Zhong, X. H. Chen and Z. Q. Zhang, *Int J Electrochem Sci.*, 13 (2018) 4338.
25. X. Y. Zheng, H. S. Lai and Z. L. Zhao, *Int J Electrochem Sci.*, 16 (2021) 150914.
26. G. Zhang, L. Wu, A. T. Tang, S. Zhang, B. Yuan, Z. C. Zheng and F. S. Pan, *Adv Mater Interfaces*, 4 (2017) 1700163.
27. H. Luo, C. F. Dong, K. Xiao and X. G. Li, *Appl Surf Sci.*, 258 (2011) 631.
28. J. Lv, T. Liang, L. Dong and W. Chen, *Corros Sci.*, 104 (2015) 144.
29. X. Yang, Y. J. Ren, S. F. Liu, Q. J. Wang and M. J. Shi, *J Cent South Univ*, 27(2020)334.
30. Y. Hou, J. Zhao, C. Q. Cheng, L. Zhang and T. S. Cao, *J Alloy Compd.*, 830 (2020) 154422.
31. D.W. Zhang, F.C. Zhou, K. Xiao, T.Y. Cui, H.C. Qian, *J Mater Eng Perform.*, 24 (2015) 2688.
32. X. Dai, H. Wang, L. K. Ju, G. Cheng, H. Cong and B. M. Z. Newby, *Int Biodeter Biodegr.*, 115 (2016) 1.